

© 2015 IEEE. Personal use of this material is permitted. Permission from IEEE must be obtained for all other uses, in any current or future media, including reprinting/republishing this material for advertising or promotional purposes, creating new collective works, for resale or redistribution to servers or lists, or reuse of any copyrighted component of this work in other works.

E. M. Bates, W. J. Birmingham and C. A. Romero-Talamás, "Development of a Bitter-Type Magnet System," in IEEE Transactions on Plasma Science, vol. 44, no. 4, pp. 540-544, April 2016, doi: 10.1109/TPS.2015.2509640.

<http://dx.doi.org/10.1109/TPS.2015.2509640>

Access to this work was provided by the University of Maryland, Baltimore County (UMBC) ScholarWorks@UMBC digital repository on the Maryland Shared Open Access (MD-SOAR) platform.

**Please provide feedback**

Please support the ScholarWorks@UMBC repository by emailing [scholarworks-group@umbc.edu](mailto:scholarworks-group@umbc.edu) and telling us what having access to this work means to you and why it's important to you. Thank you.

# Development of a Bitter-Type Magnet System

E. M. Bates, W. J. Birmingham, and C. A. Romero-Talamás

**Abstract**—A 10-T water-cooled Bitter-type magnetic system is under development at the Dusty Plasma Laboratory of the University of Maryland, Baltimore County. We present here methods used for preliminary magnet designs, which include minimizing ohmic heating and placement of water-cooling holes on current-carrying resistive Bitter conductors. Subsystems, such as the pressure vessel and vacuum chamber, motivate the coil design. The proposed power and cooling water delivery subsystems that drive and cool the magnet are also presented. A finite-element analysis is conducted on the proposed water delivery system. A one-tenth magnetic field scale-model of the magnet is currently being constructed. Upon completion and testing of the prototype magnet system, the large-scale model will be produced. Planned experiments include the propagation of magnetized waves in dusty plasma under various boundary and rotational shear flow conditions, among others in a 10-T field on a timescale of at least 10 s.

**Index Terms**—design methodology, Electromagnetic devices, optimization methods, plasma applications, Plasma devices.

## I. INTRODUCTION

A CUSTOM Bitter magnet is being designed and constructed at the University of Maryland, Baltimore County (UMBC) for magnetized dusty (complex) plasma experiments. Magnetic fields are an interesting part of the physics and science in materials, organisms, and even planetary systems. Forces from external magnetic fields in complex plasma, also called dusty plasma, produce intriguing properties on the plasma's components [1]. A goal of this magnet is to thoroughly magnetize a complex plasma, which includes the charged dust, ions, and electrons, by increasing the strength of the magnetic field and extending experimental timescales.

Magnetized dusty plasma has been investigated at a few hundred Gauss and there has been a linear trend in magnitude of the magnetic field used in experiments [2]. It was not until recently that complex plasma has been researched under relatively strong magnetic fields on the timescale of hours and even days [3], [4].

The technical hurdle of increasing the amplitude of the field is the required size of the magnet's bore, which needs to house the plasma vacuum chamber and diagnostics needed to create, stabilize, and record a plasma event. This design parameter binds the magnetic field making it a challenge to

reach stronger amplitudes. The strongest and most uniform fields published have reached around 4 T [5], [6]. The bore size in our design is constrained to the dimensions of a cylindrical bell jar handmade at UMBC. The vacuum chamber was constructed with the minimum diameter that can establish a stable dusty plasma experiment with: 1) diagnostic access; 2) 1- $\mu\text{m}$  dust grains; and 3) maximum dust displacement of confinement to the electrode at radius 0.05 m in a  $\mathbf{E} \times \mathbf{B}$  field with 2.5 V/m and 10 T, respectively. Nonmagnetic field experiments with the chamber are currently under development to ensure working conditions when manufacturing of the Bitter magnet has finished.

Most magnets at national laboratories accommodate a small bore size, on the order of millimeters, in exchange for the strongest pulsed fields seen today. There is currently no high magnetic field user facility that can host a dusty plasma experiment because of bore size and diagnostic access. This paper will address the recent advancements in the design of a Bitter-type magnet with a 0.160-m bore diameter for custom dusty plasma experimentation with programmable fields of 10 T on a timescale of 10 s to several minutes with up to 20 plasma events planned per day.

### A. Bitter Magnet

The Bitter magnet was a solution created by Francis Bitter in the 1930s [7] to solve the thermal heating problem with metal conductors in resistive magnets. The solution consisted of making the conducting magnetic turns into flat plates with cooling holes. Each conductor is separated by an insulator plate with cooling holes. Placement of the insulator on the conductors and stacking methods allows the current to travel in a helical motion as seen in Fig. 1 to create a uniform axial magnetic field. Deionized water can be sent through the cooling holes at a high flow rate to compensate for joule heating associated with high currents in metal conductors with some resistance.

### B. Magnet Design Objectives

The main objective is to have a fully functional magnet that can have programmable fields to 10 T and a maximum of 20 experiments conducted in one day. The magnet discharge from each of the 20 experiments will last for 10 s. This leaves the potential to run fewer experiments in one day with the magnet discharges lasting up to several minutes. A variable timescale is important in order to collect data for experiments and to have enough time to allow the particles to equilibrate. External magnetic fields have been used to help confine the dust, but also to effect movement on the dust [8]. Some experimenters have observed azimuthal dust

Manuscript received July 31, 2015; revised October 21, 2015 and November 18, 2015; accepted December 12, 2015. This work was supported by the Department of Mechanical Engineering, University of Maryland, Baltimore County.

The authors are with the Mechanical Engineering Department, University of Maryland, Baltimore County, Baltimore, MD 21250 USA (e-mail: evbates1@umbc.edu; birmingham2@umbc.edu; romero@umbc.edu).

Color versions of one or more of the figures in this paper are available online at <http://ieeexplore.ieee.org>.

Digital Object Identifier 10.1109/TPS.2015.2509640

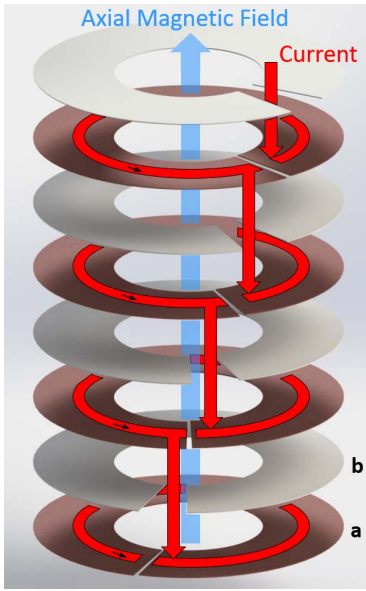


Fig. 1. Travel path of current on continuously stacked Bitter plates without cooling holes illustration. (a) Conductors. (b) Insulators.

rotation that is proportional to magnetic field strength, where ion motion and potential gradients enhanced by the magnetic field have also been observed [9]. In our setup, we plan to investigate these effects and their time for equilibration as the magnetic field ramps up and achieves steady state.

The strong magnetic field of this magnet and ramp times is justified to highly magnetize dust particle of  $1\text{-}\mu\text{m}$  diameter. At this size, the ability to optically capture plasma events at a distance where diagnostics are not affected by the rapidly changing magnetic fields is greatly increased. We are particularly interested in experiments of rotating  $\mathbf{E} \times \mathbf{B}$  drifts, including viscous heating and stability at high  $|\mathbf{E}/\mathbf{B}|$  ratios [10]. Particle tracking and temperature probes in a high field rotating dusty plasma can extend our knowledge on heating and confinement of thermonuclear fusion plasmas and rotating magnetic mirrors. Particle crystallization perpendicular to the magnetic field will also be investigated along with possible 3-D crystal formation in the presence of a high amplitude field.

The vacuum chamber is another important driving factor of the magnet's design. It must be sufficiently large to house a plasma discharge and have room for data acquisition equipment and optics. The bore of the magnet will be set to the outer diameter of the chamber. The vacuum chamber is a custom-made glass bell jar about 1.2 m in length. The bell jar can be inserted in any magnet orientation from  $0^\circ$  to  $90^\circ$ . The pressure vessel that will house the magnet will have an interface to help match a metal to glass vacuum flange without compromising vacuum. A metal collar will also be used for matching with standard vacuum components.

### C. Design: Specifications and Methods

The magnet specifications of a case study can be seen in Table I. All of the design parameters in Table I come from a differential evolution design optimization to minimize

TABLE I  
PRELIMINARY 10-T MAGNET DESIGN PARAMETERS

Total Power	2.31 MW
Resistance	23 m $\Omega$
Current	10 kA
# of Plates	257
Length	280 mm
Conductor Thickness	1 mm
Inner Radius	80 mm
Outer Radius	279 mm

ohmic heating which is implemented in Mathematica [11]. The optimization allows two different design methods to be analyzed: 1) a nested split Bitter magnet and 2) a nested solenoid Bitter magnet. In a nested design, the optimization accounts for multiple concentric coils in the magnet. Comparing the two types of magnets, a split magnet has an air gap in the center that separates the coils vertically, allowing for more optical access to the bore of the magnet at the expense of current needed to ramp the magnet to desired fields. In the solenoid design, there is no air gap, making optical access much more challenging. However, less current is needed to maintain the desired field. From the optimization results, we choose a single coil solenoid Bitter magnet with the parameters in Table I. The vacuum chamber that will be inserted into the bore of the solenoid magnet will make use of periscopes and mirrors to overcome the lacking of optical access from the side of the magnet.

A heat transfer analytical method is then used to optimally place cooling holes after the design parameters are obtained from ohmic heating optimization [12]. Placement of these cooling holes is very important to reduce the thermal load on the conducting plates. Results from this method also suggest what pressure drops are expected over the magnet's length via cooling channels (made up of both insulators and conductors when the plates are stacked). This is a very important factor in determining the dimensions for the pressure vessel as well as for the finite-element analysis (FEA) of the cooling system. Both methods will be published elsewhere detailing the processes that are used. These two methods can be continuously iterated and expanded to different case studies; design parameters can be modified to accommodate external conditions and meet off the shelf product specifications. These two methods are designed to execute faster than FEA solvers to easily change the preliminary magnet design.

### D. Power Bank System

A significant amount of power will be needed to run this system. The type of energy storage will be that of 12 V deep discharge batteries. Batteries are more favorable over other energy storage options such as capacitors and fly wheels for this dc magnet because of the high current rating, energy density, and cost. With a current rating of 10 kA, the maximum charge voltage in the system will be 230 V.

The entire system will consist of 240 batteries tied into 15 strings. Each string, consisting of 16 batteries, will be its own rack and connections will be made with bus bars.

The system will also consist of three chargers, one for every five strings. All strings will discharge 10 kA into the magnet for 10 s. The chargers will float charge the batteries with a total recharge time of 20 min after a discharge. The power bank has a design life of 10 years and will provide 200 kWh of energy storage.

#### E. Cooling Water Delivery System

FEA in ANSYS Fluent has been conducted for the proposed 10-T magnet's cooling water delivery system and has shown that a closed recirculating cooling system is an option to consider for water delivery. The proposed cooling system consists of seven 275-gal water tanks, a 7-kW water chiller, and a 700-gpm external pump. The system will be chilled to 5 °C before a magnet discharge. Nitrogen gas will also be released into the water to reduce corrosion of the copper.

This is an unsteady heat transfer problem where the high number of governing equations and boundary conditions make it hard to solve analytically. However, it must be solved because it is important to predict how the system will work given the amount of energy transfer involved. Boundary conditions representing all components of the water-cooling system are introduced into a simplified 2-D model. Many of the boundary conditions must be prescribed by ANSYS user defined functions (UDFs).

The most important boundary condition is the magnet, represented by the cooling channels in the FEA model. We apply a transient heat flux UDF boundary condition on the cooling channel's walls. The boundary condition is created to apply a heat flux over the duration of our 10-s operation time, after which the heat flux goes to zero. The logistic function is manipulated in (1) to create the ON/OFF heat flux boundary condition for the magnet as a function of time [13]

$$\text{Heat Flux (time)} = \frac{dT}{dx} = \frac{685,680}{1 + \exp(5t - 55)}. \quad (1)$$

The general process for finding the correct heat flux to apply on this boundary is as follows.

- 1) Find the average velocity in the cooling channels.
- 2) Use average velocity to find the heat transfer coefficient for noncircular holes.
- 3) Apply heat transfer coefficient in ANSYS Thermal-Electric to simulate convective heat transfer with applied current load.
- 4) Extract heat flux profile from the middle of the magnet, review maximum and minimum flux magnitudes.
- 5) Apply highest heat flux to (1).

Finding the average velocity within the cooling channels for a nonuniform pressure head on the magnet is the first step to determine (1). The average velocity determined from the momentum boundary condition for this case is 2.63 m/s.

We then use the Dittus and Boelter equation to find the heat transfer coefficient  $h$  [14]

$$h = 0.023(D_h)^{-0.2}k^{0.6}(\nu\rho)^{0.8}\left(\frac{C_p}{\mu}\right)^{0.4} \quad (2)$$

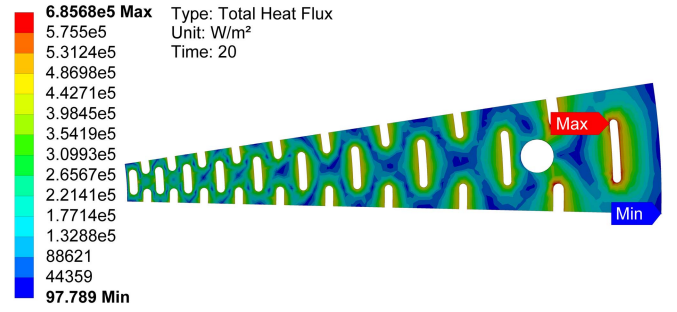


Fig. 2. 10° section of a Bitter conductor showing maximum and minimum heat flux for convective boundary conditions with applied specific heat transfer coefficient (Table II) to each radially placed cooling hole.

TABLE II  
HEAT TRANSFER COEFFICIENT FOR COOLING HOLES  
WITH DIFFERENT HYDRAULIC DIAMETERS

Radially placed cooling hole   , $h \frac{W}{m^2C}$	
Outer most hole	11598.8
2	11633.3
3	11668.4
4	11703.4
5	11738.9
6	11774.4
7	11811.0
8	11847.6
9	11884.6
Inner most hole	11925.1

where  $D_h$  is the hydraulic diameter [15]

$$D_h = \frac{4A}{P} \quad (3)$$

where  $v$  is the average velocity in the cooling channels.  $A$  and  $P$  are the area and the perimeter, respectively, of the elongated cooling hole. In Fig. 2, it can be seen that each cooling hole will have a different area and perimeter with respect to each cooling ring (holes that vary radially on a Bitter plate). Even though there are 684 cooling holes for the Bitter plate design, because of symmetry only ten holes dimensionally differ from each other. The cooling hole elongation differs but they all have the same thickness of 0.003 m. The  $h$  values are calculated for the ten different cooling holes. The 2-D FEA model represents a slice of the magnet with 20 cooling channels which include the ten different hydraulic diameter holes symmetric about the magnet's axis. Table II represents the  $h$  values for cooling holes at the outer radius to the inner radius on the Bitter plate. It is worth noting as to how the  $h$  values increase for smaller holes.

Taking these  $h$  values, we then use ANSYS thermalelectric to find the heat flux on the cooling channels' walls when our current load of 10000 A is applied to the magnet. We make a 3-D representation of our model in a computer aided design software, and scale it down to a periodic symmetric 10° slice. Then, we apply each convective cooling boundary

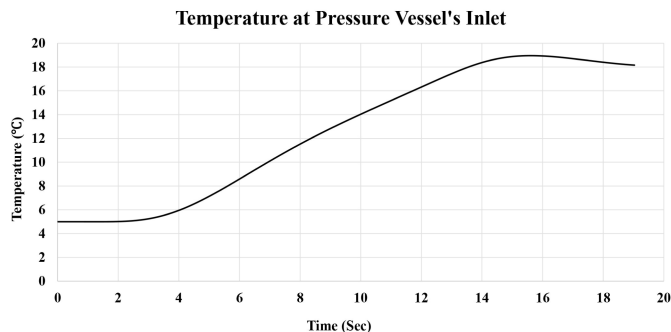


Fig. 3. Temperature at the pressure vessel's inlet versus the time of the analysis, 19 s.

from Table II to the face of each cooling hole. The results of this operation can be seen in Fig. 2. The maximum heat flux is  $685\,680\text{ W/m}^2$  and is located on the curve of the largest cooling hole. The minimum heat flux is on the outer radius of the magnet where no convective heat transfer was applied. However, there will be cooling on the outside of the magnet, but this is not considered because the cooling holes are the primary concern. The maximum heat flux is applied to the boundary condition in equation (1) to be used for every cooling channel in the ANSYS Fluent model. The maximum is used to overcompensate the actual heat generated by the magnet rather than using the average heat flux found in each individual cooling channel, if the maximum heat can be removed than so can the minimum.

The total temperature in the system is evaluated and plotted at the entry of the magnet's pressure vessel. Since this is a recirculated system, it is important that the water's temperature at this inlet can still efficiently dissipate heat at temperatures above  $5\text{ }^{\circ}\text{C}$ . The most critical time period is the first 10 s when the magnet is in operation. The temperature is plotted with respect to time in Fig. 3. For that critical time period (0–10 s), we have an inlet magnet temperature range  $5\text{ }^{\circ}\text{C}$ – $14\text{ }^{\circ}\text{C}$ . These inlet temperatures are then evaluated in the thermal optimization to find the maximum temperatures in the conductors of the magnet and of the water at the outlet of the magnet's cooling channels. This evaluation is to confirm that boiling temperature of the water is not reached, and for this case study they are not. With a  $14\text{ }^{\circ}\text{C}$  inlet water temperature, the water exiting the cooling channels will reach between  $70\text{ }^{\circ}\text{C}$  and  $80\text{ }^{\circ}\text{C}$ .

In Fig. 3, the temperature keeps increasing for another 5 s after the magnet is turned OFF. At 15 s, you can see the water chiller catching up to the temperature in the model and begins to cooling the system back down to  $5\text{ }^{\circ}\text{C}$ . The system will be back in equilibrium within 20 min; the total time it will take our battery bank to recharge.

### F. 1-T Prototype Magnet

Construction of a 1-T prototype magnet is currently in progress and will be completed in the fall of 2015. An illustration of the setup is shown in Fig. 4. The magnet will be powered by one deep charge battery for a 10-s discharge. Alternatively, an entire string of batteries can also be used to power the magnet on the order of hours. A two ton

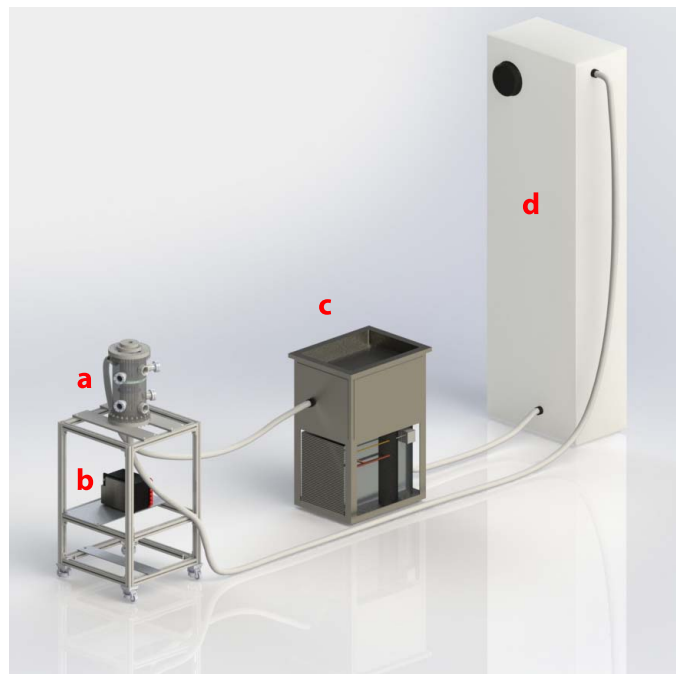


Fig. 4. 1-T prototype magnet illustration. (a) Magnet pressure vessel. (b) Battery. (c) Water chiller and pump. (d) Water storage tank.

water chiller with attached water pump will drive deionized water through the magnet at 30 gpm. One 275-gal water tank will store the deionized water. The Bitter plates are being manufactured in house with a waterjet cutter. The insulators are cut with a laser at UMBC as well. The experimental results detailing magnetic fields and temperature measurements will be published and reported at future conferences. The knowledge and experience from the prototype will be used to finalize the 10-T magnet design.

## II. CONCLUSION

The proposed 10-T resistive Bitter magnet will expand dusty plasma into new regimes, holding new opportunities for experimentation for the next 10 years. The magnet's design will be outlined through the entire design process so that other scientists can follow or modify a Bitter magnet of their own.

## REFERENCES

- [1] S. Nunomura, N. Ohno, and S. Takamura, "Effects of ion flow by  $E \times B$  drift on dust particle behavior in magnetized cylindrical electron cyclotron resonance plasma," *Jpn. J. Appl. Phys.*, vol. 36, no. 2, pp. 877–883, 1997.
- [2] L. G. D'yachkov, O. F. Petrov, and V. E. Fortov, "Dusty plasma structures in magnetic dc discharges," *Contrib. Plasma Phys.*, vol. 49, no. 3, pp. 134–147, 2009.
- [3] E. Thomas *et al.*, "The magnetized dusty plasma experiment (MDPX)," *J. Plasma Phys.*, vol. 81, no. 2, p. 345810206, 2015.
- [4] E. Thomas, Jr., R. L. Merlino, and M. Rosenberg, "Design criteria for the magnetized dusty plasma experiment," *IEEE Trans. Plasma Sci.*, vol. 41, no. 4, pp. 811–815, Apr. 2013.
- [5] E. Thomas, Jr., R. Fisher, U. Konopka, R. L. Merlino, and M. Rosenberg, "The magnetized dusty plasma experiment (MDPX) device: First observations," in *Proc. United States Nat. Committee URSI Nat. Radio Sci. Meeting*, Jan. 2014, p. 1.
- [6] M. Schwabe, U. Konopka, P. Bandyopadhyay, and G. E. Morfill, "Pattern formation in a complex plasma in high magnetic fields," *Phys. Rev. Lett.*, vol. 106, no. 21, p. 215004, 2011.
- [7] F. Bitter, "The design of powerful electromagnets part IV. The new magnet laboratory at M. I. T.," *Rev. Sci. Instrum.*, vol. 10, no. 12, pp. 373–381, 1939.

- [8] M. M. Vasil'ev, L. G. D'yachkov, S. N. Antipov, O. F. Petrov, and V. E. Fortov, "Dusty plasma structures in magnetic fields in a dc discharge," *JETP Lett.*, vol. 86, no. 6, pp. 358–363, 2007.
- [9] N. Sato, G. Uchida, T. Kaneko, S. Shimizu, and S. Iizuka, "Dynamics of fine particles in magnetized plasmas," *Phys. Plasmas*, vol. 8, no. 5, p. 1786, 2000.
- [10] O. Ishihara and N. Sato, "On the rotation of a dust particulate in an ion flow in a magnetic field," *IEEE Trans. Plasma Sci.*, vol. 29, no. 2, pp. 179–181, Apr. 2001.
- [11] *Mathematica 9*, Wolfram Res., Champaign, IL, USA, 2013.
- [12] W. J. Birmingham, E. M. Bates, and C. A. Romero-Talamás, "Analytic thermal design of bitter-type solenoids," *J. Thermal Sci. Eng. Appl.*, vol. 8, no. 2, p. 021008, 2015.
- [13] D. W. Hosmer, Jr., S. Lemeshow, and R. X. Sturdivant, *Applied Logistic Regression*. New York, NY, USA: Wiley, 2013.
- [14] A. J. Chapman, *Heat Transfer*, 4th ed. New York, NY, USA: Macmillan Publ. Co., 1984, ch. 8.
- [15] W. M. Kays and M. E. Crawford, *Convective Heat and Mass Transfer*, 3rd ed. New York, NY, USA: McGraw-Hill, 1993, ch. 14.

Authors' photographs and biographies not available at the time of publication.